Visnyk NTUU KPI Seriia – Radiotekhnika Radioaparatobuduvannia, 2026, Iss. 103, pp. 51–60

UDC 621.396.96

Multitarget Tracking Algorithm With Joint Probabilistic Data Association Using Coordinate and Amplitude Information

Kovtun I. S., Zhuk S. Ya.

National Technical University of Ukraine "Ihor Sikorsky Kyiv Polytechnic Institute", Kyiv, Ukraine

E-mail: *i.kovtun.rtf@kpi.ua, s.zhuk@kpi.ua*

The widespread use of small Unmanned Aerial Vehicles (UAVs) makes the task of their tracking highly relevant, especially in conditions where objects are at close ranges and their trajectories intersect. Frequency-Modulated Continuous-Wave (FMCW) radar is a modern tool for detecting and tracking small UAVs, allowing for a significant reduction in peak transmit power, thus lowering energy consumption and improving the weight, size, and cost characteristics of the system. Small UAVs have extremely low radar cross-section values. Increasing the detection range of small UAVs by FMCW radar can be achieved by lowering the detection threshold, which, however, leads to a significant increase in the probability of false alarms. To improve the efficiency of multitarget tracking using FMCW radar data in the presence of a significant number of false alarms, the Amplitude-Aided Joint Probabilistic Data Association Filter (AA-JPDAF) algorithm has been developed. This algorithm proposes the use of decision statistics (amplitude information) from the output of the optimal primary signal processing receiver as additional information. This information is utilised at the data association stage based on the Joint Probabilistic Data Association (JPDA) method. Target motion parameter estimation for each trajectory is performed using the Extended Kalman Filter (EKF). The analysis of the AA-JPDAF algorithm and its comparison with the conventional JPDAF were conducted via statistical simulation for scenarios involving intersecting trajectories and long-term parallel motion of targets at close ranges.

Keywords: FMCW radar; UAV; multitarget tracking; false alarms; joint probabilistic data association; Kalman filter; posterior probability; decision statistics; signal-to-noise ratio; track loss

DOI: 10.64915/RADAP.2026.103.51-60

Introduction

One of the key tasks of airspace radar monitoring is tracking small aerial objects, primarily unmanned aerial vehicles (UAVs). The relevance of this task is driven by a significant increase in the production of small UAVs and the rising threat level [1, 2] associated with their widespread use. In practice, a typical contemporary scenario involves the simultaneous observation of not only several individual UAVs but also swarms [3], where objects may be located at close ranges and their trajectories may intersect.

Recently, significant interest has emerged in Frequency-Modulated Continuous-Wave (FMCW) radars with continuous linear frequency modulation [4]. FMCW radars enable a substantial reduction in peak transmit power, thereby lowering energy consumption and improving the weight, size, and cost characteristics of the system. This extends their applicability to sites unsuitable for conventional surveillance radars.

Small UAVs, as radar observation targets, are characterised by radar cross-section values on the order of 0.01–0.5 m^2 [5], which significantly complicates the tasks of detection and tracking. One of the key approaches to extending the detection range of small UAVs by radar systems is the reduction of the detection threshold [6]. However, this inevitably leads to an increase in the false alarm probability, which may reach values of $F = 10^{-3}$ or higher.

In secondary data processing, the following primary tasks are traditionally addressed: target track initiation, track maintenance (tracking), track termination (deletion), and kinematic calculations for radar data end-users [7, 8]. The track initiation task enables a decision regarding the presence of a target within the radar's surveillance region with a specified probability prior to its handover for tracking. At the track initiation stage, the problem of optimal estimation for trajectory parameters is generally not addressed in order to minimize computational overhead. Therefore, the number of targets being tracked during each radar scan is considered known.

In the presence of a large number of false measurements, decision statistics (amplitude

information) obtained from the output of the optimal primary signal processing receiver have been proposed as additional information to improve target trajectory tracking [9, 10]. In [11], an adaptive radar tracking algorithm for a manoeuvring UAV was synthesised using Probabilistic Data Association (PDA) based on both coordinate and amplitude features. The use of amplitude information improves the reliability of measurement association and reduces the impact of false measurements on the tracking process.

In multitarget tracking under conditions of a high false measurement density, the Joint Probabilistic Data Association (JPDA) algorithm has gained widespread use as a multi-trajectory extension of the single-trajectory PDA algorithm [12]. JPDA analyses all feasible sets of trajectory-measurement pairs formed through the gating process and calculates their posterior probabilities, which are subsequently used to estimate the motion parameters of targets for each trajectory.

The JPDA data association algorithm can be combined with various target motion estimation algorithms. The primary and most fundamental approach is the Joint Probabilistic Data Association Filter (JPDAF), in which the JPDA method is integrated with the Kalman filter. When the target motion and measurement models are linear, a Linear Kalman Filter (LKF) is employed; when nonlinearities are present, the models are linearised, and an Extended Kalman Filter (EKF) is used [7].

In the conventional JPDAF tracking algorithm, decision statistics from the output of the optimal primary signal processing receiver are not utilised. Consequently, the development of a multitarget tracking algorithm for FMCW radar data, specifically a JPDAF incorporating amplitude information — hereafter referred to as the Amplitude-Aided Joint Probabilistic Data Association Filter (AA-JPDAF) — represents a relevant and timely research problem.

1 Problem Statement

To describe the motion trajectory of the i-th target $i = \overline{1,N}$ in a Cartesian coordinate system, a linear stochastic dynamic system is employed [8]:

$$\mathbf{u}_i(k) = \mathbf{F}(k,k-1)\mathbf{u}_i(k-1) + \mathbf{G}(k)\omega_i(k), \qquad (1)$$

where: $\mathbf{u}_i(k)$ is a vector containing the motion parameters of the i-th target along the axes of the coordinate system; $\mathbf{F}(k,k-1)$, $\mathbf{G}(k)$ are known matrices; $\omega_i(k)$ is uncorrelated excitation noise with zero mean and covariance matrix $Q(k)$.

The FMCW radar measurement equation in a spherical coordinate system is nonlinear and can be expressed as [8]:

$$\mathbf{u}_i^{\upsilon}(k) = \mathbf{h}(\mathbf{u}_i(k)) + \upsilon_i(k), \qquad (2)$$

where $\mathbf{u}_i^{\upsilon}(k)$ is the measurement vector of the i-th target $i = \overline{1,N}$, containing its measured coordinates in the spherical system; $\mathbf{h}(\cdot)$ is a known vector-valued nonlinear measurement function, and $\upsilon_i(k)$ – denotes the measurement noise with a covariance matrix $\mathbf{R}_i(k)$.

Equation (2) facilitates the description of various measurement acquisition scenarios for both two-dimensional and three-dimensional FMCW radars.

To enhance the tracking efficiency of small UAVs in the presence of false measurements, it is proposed to use decision statistics from the output of the optimal primary signal processing receiver as additional information. During each scan, the optimal receiver performs target detection by comparing the decision statistics $\tilde{z}(k)$ in a resolution cell with an input threshold. If a detection occurs, a measurement is formed; the coordinate information characterises its position in the surveillance area, and the value of the obtained decision statistics $\tilde{z}(k)$ is also retained.

For secondary trajectory processing, it is more convenient to utilise normalised decision statistics $z(k) = \tilde{z}(k)/\sigma_n$, where σ_n is the RMS noise at the receiver input. When using an FMCW radar, the probability density of the normalised decision statistics in the presence of a target, $f_S(z(k))$ follows a noncentral chi-square distribution $\chi_2'^2(q)$ with two degrees of freedom and noncentrality parameter q, which is equal to the Signal-to-Noise Ratio (SNR) [13]. In the absence of a target, the probability density of the decision statistics $f_N(z(k))$ follows a central chi-square distribution χ_2^2 with two degrees of freedom. The normalised decision statistics in each resolution cell are compared with a normalised input threshold $H = -2\ln F$. The decision statistics that exceed this threshold are then described by truncated probability density functions $f_S^{\text{y}}(z(k))$ and $f_N^{\text{y}}(z(k))$, which are defined as:

$$f_S^{\text{y}}(z(k)) = \frac{f_S(z(k))}{D}; \qquad (3)$$

$$f_N^{\text{y}}(z(k)) = \frac{f_N(z(k))}{F}, \qquad (4)$$

where D and F are the probabilities of correct detection and false alarm, respectively, defined as:

$$D = \int_H^{\infty} f_S(z(k))dz(k); \qquad (5)$$

$$F = \int_H^{\infty} f_N(z(k))dz(k). \qquad (6)$$

In the synthesis of the algorithm, the following assumptions are adopted [7]:

1. A known and previously estimated number of targets N is present within the surveillance region.

2. Each target can generate at most one measurement within the surveillance region at each scan.

3. Each measurement can originate from at most one target.

4. Measurements generated by one target may fall within the validation gate of another target.

5. The probability of target detection is D. The probability that a true measurement falls within the corresponding validation gate is P_s.

6. The number of false measurements within the surveillance region follows a Poisson distribution with known spatial density λ. The spatial distribution of false measurements over the surveillance region is uniform.

7. The SNR q is assumed to be known and constant over time.

2 Development of a Multitarget Tracking Algorithm with Joint Probabilistic Data Association Using Coordinate and Amplitude Information

2.1 Gating of measurements for a group of targets and calculation of conditional state estimates based on validated measurements

In accordance with the synthesis methodology for the JPDAF algorithm [7], the input data consist of the estimates of the motion parameter vectors $\hat{\mathbf{u}}_i(k-1)$ and the corresponding error covariance matrices $\hat{\mathbf{P}}_i(k-1)$ for each target $i = \overline{1,N}$. These values, calculated at step $k-1$, incorporate the sequence of measured coordinates $\mathbf{U}^{\upsilon}(k-1) = \mathbf{u}^{\upsilon}(1),\ldots,\mathbf{u}^{\upsilon}(k-1)$ and the decision statistics of the measurements $\mathbf{Z}(k) = \mathbf{z}(1),\ldots,\mathbf{z}(k-1)$ obtained up to and including time instant $k-1$. For each target $i = \overline{1,N}$ the predicted state vector $\mathbf{u}_i^*(k)$ and the corresponding prediction error covariance matrix $\mathbf{P}_i^*(k)$ are computed as:

$$\mathbf{u}_i^*(k) = \mathbf{F}_i(k,k-1)\hat{\mathbf{u}}_i(k-1); \tag{7}$$

$$\begin{aligned}\mathbf{P}_i^*(k) = \mathbf{F}_i(k,k-1)\hat{\mathbf{P}}_i(k-1){\mathbf{F}_i}^T(k,k-1)+\\ +\mathbf{G}(k)\mathbf{Q}(k)\mathbf{G}^T(k).\end{aligned} \tag{8}$$

For each target $i = \overline{1,N}$ a set of candidate measurements is obtained through the gating process. The test for whether the m-th measurement $\mathbf{u}_m^{\upsilon}(k)$ falls within the validation gate of the i-th target is performed by checking the condition:

$$\rho_{im}(k) = ||\,\mathbf{u}_m^{\upsilon}(k) - \mathbf{H}(\mathbf{u}_i^*(k))||_{\mathbf{D}_i(k)} \le \gamma, \tag{9}$$

where $\rho_{im}(k)$ is a quadratic form defined as

$$\begin{aligned}||\,\mathbf{u}_m^{\upsilon}(k) - \mathbf{H}(\mathbf{u}_i^*(k))||_{\mathbf{D}_i(k)} =\\ = {\mathbf{r}_{im}}^T(k)\mathbf{D}_i^{-1}(k)\mathbf{r}_{im}(k),\end{aligned} \tag{10}$$

where $\mathbf{r}_{im}(k) = \mathbf{u}_m^{\upsilon}(k) - \mathbf{H}(\mathbf{u}_i^*(k))$ is the innovation (residual) vector; $\mathbf{H}(\mathbf{u}_i^*(k))$ is the Jacobian matrix of the vector-valued function $\mathbf{h}(\cdot)$ evaluated at $\mathbf{u}_i^*(k)$; $\mathbf{D}_i(k)$ is the innovation covariance matrix for measurement $\mathbf{u}_m^{\upsilon}(k)$ when associated with the i-th trajectory, calculated as:

$$\mathbf{D}_i(k) = \mathbf{H}_i(k)\mathbf{P}_i^*(k)\mathbf{H}_i^T(k) + \mathbf{R}_i(k); \tag{11}$$

γ is the gating threshold, determined by a predefined probability P_{s} of the true target measurement falling within the gate [14].

Based on the results of analysing the inclusion of measurements within the individual validation gates of all targets, a measurement vector $\mathbf{u}^{\upsilon T}(k) = (\mathbf{u}_1^{\upsilon}(k),\ldots,\mathbf{u}_M^{\upsilon}(k))$ is formed, which contains the coordinate information of the measurements, where M is the number of measurements that fall within the validation gates of the targets at time step k. In addition, the vector $\mathbf{z}(k) = (z_1(k),\ldots,z_M(k))$ is formed, which includes the decision statistics of the obtained measurements. A gating matrix $\mathbf{C}(k)$ of dimension is defined with binary elements:

$$c_{i\,m} = \begin{cases} 1, & \rho_{im}(k) \le \gamma, \quad i = \overline{1,N},\ m = \overline{1,M};\\ 0, & \rho_{im}(k) > \gamma. \end{cases} \tag{12}$$

The conditional state estimates $\tilde{\mathbf{u}}_{im}(k)$ and the corresponding error covariance matrices $\tilde{P}_i(k)$ for target $i = \overline{1,N}$ based on validated measurements $m = \overline{1,M}$ (where $c_{i\,m} = 1$) are calculated as:

$$\tilde{\mathbf{u}}_{im}(k) = \mathbf{u}_i^*(k) + \mathbf{K}_i(k)(\mathbf{u}_m^{\upsilon}(k) - \mathbf{H}(\mathbf{u}_i^*(k))); \tag{13}$$

$$\begin{aligned}\mathbf{K}_i(k) = \mathbf{P}_i^*(k)\mathbf{H}^T(\mathbf{u}_i^*(k))\times\\ \times\left(\mathbf{H}(\mathbf{u}_i^*(k))\mathbf{P}_i^*(k)\mathbf{H}^T(\mathbf{u}_i^*(k)) + \mathbf{R}_i\right)^{-1};\end{aligned} \tag{14}$$

$$\tilde{\mathbf{P}}_i(k) = \mathbf{P}_i^*(k) - \mathbf{K}_i(k)\mathbf{H}(\mathbf{u}_i^*(k))\mathbf{P}_i^*(k). \tag{15}$$

As demonstrated by formulae (14) and (15), the error covariance matrices $\tilde{\mathbf{P}}_i(k)$ are independent of the actual measurement values $m = \overline{1,M}$.

2.2 Formulation of the set of joint association hypotheses and calculation of their posterior probabilities

For each target $i = \overline{1,N}$ we associate discrete random variables $\theta_i(k)$, which take values $m_i = \overline{0,M}$, to characterise the feasible data association scenarios [12]:

- $\theta_i(k) = m_i$, $m_i = \overline{1,M}$: represents the event that measurement m_i originates from the target i;

- $\theta_i(k) = 0$: represents the event that no measurement originates from target i (a target miss or misdetection).

The measurement indices m_i, with which the i-th target can be associated are determined based on the gating matrix $\mathbf{C}(k)$. To describe thejoint association of measurements with trajectories at step k, a random vector $\theta(k) = (\theta_1(k), \ldots, \theta_N(k))$ is utilised. The random event $\theta(k) = (m_1, \ldots, m_N)$ describes a particular joint association hypothesis of measurements to trajectories. Taking into account the constraints introduced in Section 1, for the vector elements $\theta(k)$, if $i \neq j$, the condition $m_i \neq m_j$ must be satisfied for all $m_i \neq 0$ and $m_j \neq 0$.

To compute all possible feasible joint association scenarios, it is appropriate to consider the random events $\theta(k) = (m_1, \ldots, m_N)$ in an equivalent form as hypotheses $H_l(k)$, $l = \overline{1,L}$. Each hypothesis $H_l(k)$ can be mapped with an association matrix $\mathbf{A}_l(k)$ of dimension. Its rows $i = \overline{1,N}$ correspond to target trajectories, while the first column ($m = 0$) represents target misses. Columns $m = \overline{1,M}$ correspond to the obtained measurements. Binary elements of the matrix a_{im} , $i = \overline{1,N}, m = \overline{1,M}$ describe the events of specific measurement-to-target assignments:

$$a_{i\,m} = \begin{cases} 1, & \text{target } i \text{ is associated} \\ & \text{with measurement } m, \\ 0, & \text{target } i \text{ is not associated} \\ & \text{with measurement } m. \end{cases}$$

The binary elements a_{i0} , $i = \overline{1,N}$ describe events regarding target detection:

$$a_{i\,0} = \begin{cases} 1, & \text{target is missed (no} \\ & \text{associated measurement),} \\ 0, & \text{a measurement for target } i \text{ is present.} \end{cases}$$

The following constraints are applied to the matrix elements:

1. At most one measurement per target:

$$\sum_{m=0}^{M} a_{im} = 1 \ \text{ for all } \ i = \overline{1,N}. \tag{16}$$

2. At most one target per measurement:

$$\sum_{i=1}^{N} a_{im} \leq 1 \ \text{ for all } \ m = \overline{1,M}. \tag{17}$$

To determine all possible association matrices $H_l(k)$, $l = \overline{1,L}$ various approaches are employed, including exhaustive combinatorial enumeration of feasible hypotheses [14], m-best assignment algorithms [15], as well as graph-based data association methods with preliminary measurement gating [16]. In this process, the gating matrix $\mathbf{C}(k)$ is utilised and the constraints given by (16) and (17) are taken into account. It should also be noted that for each association matrix $\mathbf{A}_l(k)$, an equivalent hypothesis $H_l(k)$ is defined by the tuple $i = \overline{1,N}$ of the vector $\theta(k)$.

Using the association matrix $\mathbf{A}_l(k)$ the following indicators can be computed for each hypothesis $H_l(k)$:

- a binary indicator of trajectory association:

$$\delta_i^l = \sum_{m=1}^{M} a_{im} \leq 1, \tag{18}$$

which demonstrates whether any of the measurements were associated with trajectory under hypothesis $\theta_l(k)$, and takes the value 1, if such a measurement exists, or 0 if a measurement corresponding to the target was not found;

- a binary indicator of measurement association:

$$\tau_m^l = \sum_{i=1}^{N} a_{im} \leq 1, \tag{19}$$

which reflects whether any target was associated with measurement within hypothesis $\theta_l(k)$, and takes the value 1 if such a target exists, or 0 otherwise.

With consideration of (19), the number of false (not associated with trajectories) measurements φ^l in hypothesis $\theta_l(k)$, is determined by the formula:

$$\varphi^l = \sum_{m=1}^{M} (1 - \tau_m^l). \tag{20}$$

The next step is the calculation of conditional posterior probabilities $P(\,H_l(k)|\mathbf{U}^{\upsilon}(k), \mathbf{Z}(k)), l = \overline{1,L}$ for the hypotheses $H_l(k)$. Posterior probabilities $P(\,H_l(k)|\mathbf{U}^{\upsilon}(k), \mathbf{Z}(k)), l = \overline{1,L}$ are calculated based on Bayes' formula:

$$P(\,H_l(k) \mid \mathbf{U}^{\upsilon}(k), \mathbf{Z}(k)) = \frac{\mathcal{L}_l(k)\, P(H_l(k))}{C(k)}, \tag{21}$$

where $\mathcal{L}_l(k) = f(\mathbf{u}^{\upsilon}(k), \mathbf{z}(k) \mid H_l(k), \mathbf{U}^{\upsilon}(k-1), \mathbf{Z}(k-1))$ is the likelihood function of hypothesis $H_l(k)$; $P(H_l(k))$ is the prior probability of hypothesis $H_l(k)$; $C(k) = f(\mathbf{u}^{\upsilon}(k), \mathbf{z}(k) \mid \mathbf{U}^{\upsilon}(k-1), \mathbf{Z}(k-1))$ is the normalising factor:

$$\begin{aligned} C(k) &= f(\mathbf{u}^{\upsilon}(k), \mathbf{z}(k) \mid \mathbf{U}^{\upsilon}(k-1), \mathbf{Z}(k-1)) = \\ &= \sum_{l=1}^{L} \mathcal{L}_l(k) P(H_l(k)). \end{aligned} \tag{22}$$

The likelihood function $\mathcal{L}_l(k)$ is calculated according to the expression

$$\begin{aligned}\mathcal{L}_l(k) &= f(\mathbf{u}^{\upsilon}(k), \mathbf{z}(k) \mid H_l(k), \mathbf{U}^{\upsilon}(k-1), \mathbf{Z}(k-1)) = \\ &= \prod_{i=1}^{N} \left(\Lambda_{im_i}(k) f_S^{\mathrm{y}}(z_{m_i}(k))\right)^{\delta_i^l} \times \\ &\quad \times \prod_{m=1}^{M} \left(V^{-1} f_N^{\mathrm{y}}(z_m(k))\right)^{1-\tau_m^l} = \\ &= V^{-\varphi^l} \prod_{i=1}^{N} \left(\Lambda_{im_i}(k) f_S^{\mathrm{y}}(z_{m_i}(k))\right)^{\delta_i^l} \times \\ &\quad \times \prod_{m=1}^{M} \left(f_N^{\mathrm{y}}(z_m(k))\right)^{1-\tau_m^l}.\end{aligned} \tag{23}$$

Here $\Lambda_{im_i}(k)$ is the likelihood function of associating the measured coordinates $\mathbf{u}_{m_i}^{\upsilon}(k)$ of measurement m_i with trajectory i, which is Gaussian [14] and given by

$$\begin{aligned}\Lambda_{im_i}(k) &= (2\pi)^{-1} \det(\mathbf{D}_i(k))^{-1/2} \times \\ &\quad \times \exp\left\{-0.5 \,||\, \mathbf{u}_{m_i}^{\upsilon}(k) - \mathbf{H}(\mathbf{u}_i^*(k))||_{\mathbf{D}_i(k)}\right\}.\end{aligned} \tag{24}$$

The parameter V denotes the volume of the validation gate at the k-th scan.

The first product in (23) calculates the likelihoods of measurements associated with the corresponding trajectories. For such measurements $\delta_i^l = 1$. The measurement index m_i associated with the i-th target is determined by the ordered tuple $i = \overline{1,N}$ of the vector $\theta(k)$ corresponding to hypothesis $H_l(k)$. The second product in formula (23) calculates the likelihood of false measurements that are not associated with targets in hypothesis $H_l(k)$.

The prior probabilities $P(H_l(k))$, $l = \overline{1,L}$, are calculated according to formula [14]:

$$P(H_l(k)) = \frac{\varphi^l!}{M!} \prod_{i=1}^{N} (DP_s)^{\delta_i^l} (1 - DP_s)^{1-\delta_i^l} P_\lambda(\varphi^l), \tag{25}$$

where $P_\lambda(\varphi^l)$ is the Poisson distribution:

$$P_\lambda(\varphi^l) = \frac{(\lambda V)^{\varphi^l}}{\varphi^l!} e^{-\lambda V}. \tag{26}$$

Substituting the likelihood function (23) and the prior probability (25) into the Bayesian formula (21), the posterior probability of the joint hypothesis is obtained as:

$$\begin{aligned}P(\, H_l(k) \,|\mathbf{U}^{\upsilon}(k), \mathbf{Z}(k)) &= \\ &= C^{-1} \prod_{i=1}^{N} \left(\Lambda_{im_i}(k) f_S^{\mathrm{y}}(z_{m_i}(k))\right)^{\delta_i^l} \times \\ &\quad \times \prod_{m=1}^{M} \left(f_N^{\mathrm{y}}(z_m(k))\right)^{1-\tau_m^l} \lambda^{\varphi^l} \times \\ &\quad \times \prod_{i=1}^{N} (DP_s)^{\delta_i^l} (1 - DP_s)^{1-\delta_i^l}.\end{aligned} \tag{27}$$

where C is a normalising constant calculated as:

$$\begin{aligned}C &= \sum_{l=1}^{L} \prod_{i=1}^{N} \left(\Lambda_{im_i}(k) f_S^{\mathrm{y}}(z_{m_i}(k))\right)^{\delta_i^l} \times \\ &\quad \times \prod_{m=1}^{M} \left(f_N^{\mathrm{y}}(z_m(k))\right)^{1-\tau_m^l} \lambda^{\varphi^l} \times \\ &\quad \times \prod_{i=1}^{N} (DP_s)^{\delta_i^l} (1 - DP_s)^{1-\delta_i^l} = \\ &= f(\mathbf{u}^{\upsilon}(k), \mathbf{z}(k) \mid \mathbf{U}^{\upsilon}(k-1), \mathbf{Z}(k-1)) \times \\ &\quad \times M(k)!\, e^{\lambda V}.\end{aligned} \tag{28}$$

2.3 Determination of association probabilities and unconditional motion state estimates

In accordance with the JPDAF algorithm synthesis methodology [7, 12] the probability $\beta_{i\,m}(k)$ of associating the m-th measurement with the i-th target (the event $\theta_i = m$) is calculated by summing the posterior probabilities of all joint hypotheses $P(\, H_l(k) | \mathbf{U}^{\upsilon}(k), \mathbf{Z}(k))$ in which this specific association occurs:

$$\beta_{i\,m}(k) = \sum_{l=1, \theta_i = m}^{L} P(\, H_l(k) | \mathbf{U}^{\upsilon}(k), \mathbf{Z}(k)). \tag{29}$$

The probability of a target miss (misdetection) for target is defined as:

$$\beta_{i0}(k) = 1 - \sum_{m=1}^{M} \beta_{i\,m}(k). \tag{30}$$

The calculation of the resulting state vector estimates and the error covariance matrix for each trajectory is performed by considering all the validated association hypotheses in which it participates:

$$\hat{\mathbf{u}}_i(k) = \mathbf{u}_i^*(k) \beta_{i0}(k) + \sum_{m=1}^{M} \hat{\mathbf{u}}_{im}(k) \beta_{i\,m}(k); \tag{31}$$

$$\begin{aligned}\hat{\mathbf{P}}_i(k) &= \Big\{\mathbf{P}_i^*(k) + (\mathbf{r}_i^*(k) - \hat{\mathbf{r}}_i(k)) \times \\ &\quad \times (\mathbf{r}_i^*(k) - \hat{\mathbf{r}}_i(k))^T\Big\} \beta_{i0}(k) + \\ &\quad + \sum_{m=1}^{M} \Big\{\tilde{\mathbf{P}}_i(k) + (\hat{\mathbf{r}}_{im}(k) - \hat{\mathbf{r}}_i(k)) \times \\ &\quad \times (\hat{\mathbf{r}}_{im}(k) - \hat{\mathbf{r}}_i(k))^T\Big\} \beta_{i\,m}(k).\end{aligned} \tag{32}$$

As follows from equation (31), the position correction for each target is performed not based on a single measurement, but on a weighted average combination of all associated measurements.

Thus, in the multi-target tracking algorithm AA-JPDAF developed in Section 2 for FMCW radar data,

amplitude information from the output of the optimal primary signal processing receiver is utilised during the calculation of posterior hypothesis probabilities $P(H_l(k)|\mathbf{U}^{\upsilon}(k), \mathbf{Z}(k))$ according to equation (27).

3 Performance Analysis of the Developed Algorithm

The performance of the developed multitarget tracking algorithm with joint probabilistic data association using coordinate and amplitude information was analysed using the example of a two-coordinate FMCW radar measuring target range and azimuth. To describe the evolution of target motion parameters along the axes of a rectangular coordinate system, a second-order polynomial model was employed. In this case, the state vector of the i-th target, $\mathbf{u}_i{}^T(k) = (x_i(k), \dot{x}_i(k), \ddot{x}_i(k), y_i(k), \dot{y}_i(k), \ddot{y}_i(k))$, includes the coordinates of position, velocity, and acceleration along the respective axes.

For this model, the state transition matrix $\mathbf{F}$ and the process noise gain matrix $\mathbf{G}$ are given by:

$$\mathbf{F} = \begin{bmatrix} 1 & T & \frac{T^2}{2} & 0 & 0 & 0 \\ 0 & 1 & T & 0 & 0 & 0 \\ 0 & 0 & 1 & 0 & 0 & 0 \\ 0 & 0 & 0 & 1 & T & \frac{T^2}{2} \\ 0 & 0 & 0 & 0 & 1 & T \\ 0 & 0 & 0 & 0 & 0 & 1 \end{bmatrix}, \tag{33}$$

$$\mathbf{G} = \begin{bmatrix} \frac{aT^3}{6} & 0 \\ \frac{aT^2}{2} & 0 \\ aT & 0 \\ 0 & \frac{aT^3}{6} \\ 0 & \frac{aT^2}{2} \\ 0 & aT \end{bmatrix}. \tag{34}$$

In these expressions, a represents the standard deviation (RMS) of the rate of change of the target's acceleration. For the simulation, the parameters were set to $T = 1$ s, $a = 2$ m/s^3.

The linearised measurement equation of the two-coordinate FMCW radar in the Cartesian coordinate system has the form [17]

$$\mathbf{u}_i^{\upsilon}(k) = \mathbf{H}\mathbf{u}_i(k) + \upsilon_i(k), \tag{35}$$

where $\mathbf{u}_i^{\upsilon}(k) = (x_i^{\upsilon}(k), y_i^{\upsilon}(k))^T$ is the observation vector containing the measured Cartesian position coordinates of the small UAV. The vector $\upsilon_i(k) = (\upsilon_{ix}(k), \upsilon_{iy}(k))^{\mathrm{T}}$ represents the measurement error vector with the corresponding error covariance matrix.

$$\mathbf{R}_i(k) = \begin{bmatrix} \sigma_{ix}^2(k) & \sigma_{ixy}^2(k) \\ \sigma_{ixy}^2(k) & \sigma_{iy}^2(k) \end{bmatrix}. \tag{36}$$

The elements of the correlation matrix $\mathbf{R}_i(k)$ are determined by the formulas:

$$\sigma_{ix}^2(k) = \sigma_r^2 \cos^2\beta_i(k) + r_i^2(k)\sigma_\beta^2 \sin^2\beta_i(k); \tag{37}$$

$$\sigma_{iy}^2(k) = \sigma_r^2 \sin^2\beta_i(k) + r_i^2(k)\sigma_\beta^2 \cos^2\beta_i(k); \tag{38}$$

$$\sigma_{ixy}^2(k) = 0.5 \sin 2\beta_i(k)(\sigma_r^2 - r_i^2(k)\sigma_\beta^2), \tag{39}$$

where σ_r^2 and σ_β^2 are the variances of the measurement errors of the target coordinates in the spherical coordinate system; $r(k)$ and $\beta(k)$ are the target coordinates in the polar coordinate system. In the simulation, the RMS of the range measurement error was set as $\sigma_r = 2$ m, and for the azimuth, $\sigma_\beta = 1°$.

Algorithm performance evaluation was conducted using statistical indicators of the probabilities of key tracking events, specifically [7, 18–20]:

- Probability of track loss, P_{lost} (True Lost): represents cases where the trajectory began to track exclusively false measurements, having lost association with the object.
- Probability of divergence, $P_{\text{divergence}}$: characterises a critical growth of the validation gate (exceeding initial dimensions by more than 3 times), which makes further tracking impractical.
- Probability of switching, P_{switch}: represents situations where the original target is lost and the filter switches to tracking a different target.
- Probability of mutual swap, P_{swap}: demonstrates a situation where, after gates intersect, the filters mutually exchange targets and continue subsequent tracking.

3.1 Scenario of rectilinear motion of two targets with intersecting trajectories

As the first scenario, rectilinear motion of two targets with intersecting trajectories is considered (Fig. 1). The trajectory intersection occurs at an angle of 40 degrees [19, 20]. Experiments were conducted for identical Signal-to-Noise Ratio (SNR) values for both targets: (14 dB, 14 dB) and (15 dB, 15 dB). The detection probabilities for SNR values of 14 dB and 15 dB are shown in Fig. 2. The study was conducted using the Monte Carlo method based on 1000 trials.

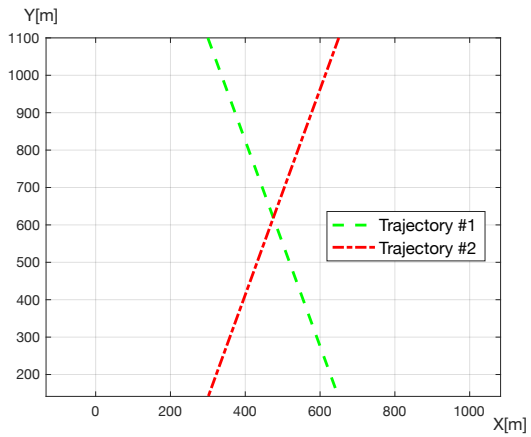

Fig. 1. Trajectories of motion of two targets.

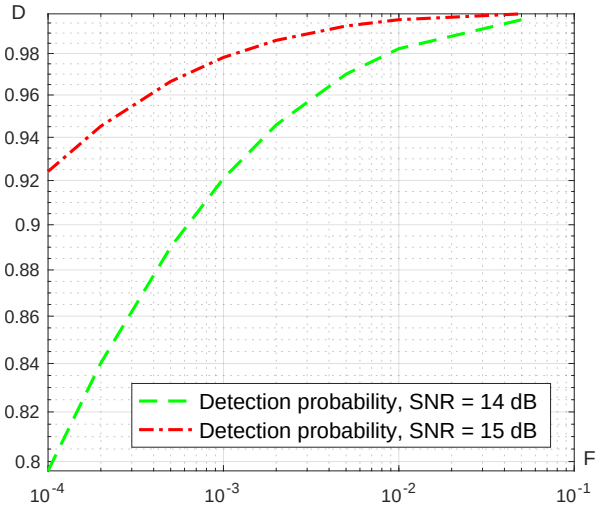

Fig. 2. Target detection probability.

Figures 3 and 4 present the results of experiments with the known JPDAF algorithm.

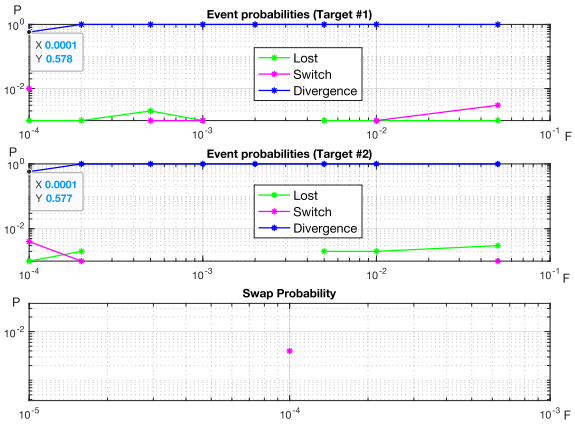

Fig. 3. Tracking event probabilities for JPDAF, SNR (14 dB, 14 dB).

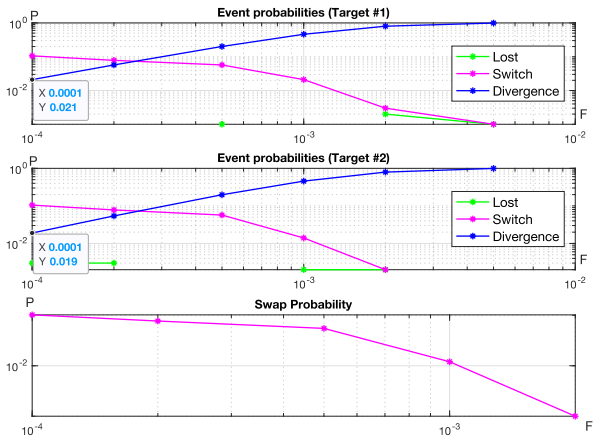

Fig. 4. Tracking event probabilities for JPDAF, SNR (15 dB, 15 dB).

The simulation results for the developed AA-JPDAF algorithm for a pair of targets with an SNR of (14 dB, 14 dB) are shown in Fig. 5. The use of amplitude information from the reports allowed for a significant improvement in tracking characteristics: the combined probability $P_{\text{lost}} + P_{\text{divergence}}$ does not exceed 1%, even at a false alarm probability of $F = 0.005$. Specifically, $P_{\text{divergence}}$ is less than 0.1%, while P_{lost} is up to 0,5%.

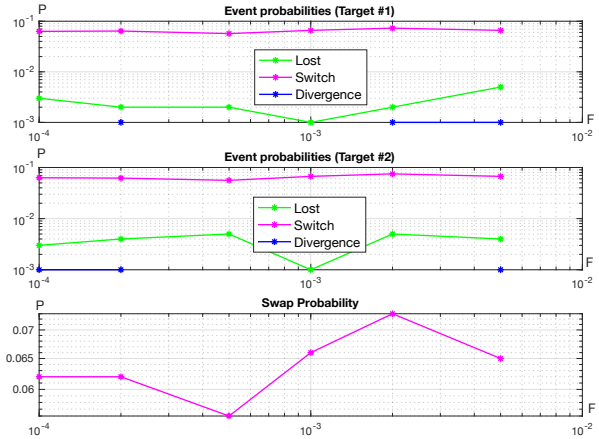

Fig. 5. Tracking event probabilities for AA-JPDAF, SNR (14 dB, 14 dB).

The switching indicators for the trajectories remain consistently low: $P_{\text{divergence}} \leq 7.5\%$, while the probability of mutual target swap (P_{swap}) fluctuates within the range of 5.6%...7.3%. Consequently, in the scenario with intersecting trajectories, the AA-JPDAF algorithm demonstrates improved tracking performance compared to the JPDAF algorithm.

3.2 Scenario with complex motion trajectories

Of particular interest is the ability of tracking algorithms to handle closely spaced targets. Therefore, to evaluate algorithm performance, the scenario proposed in [20] was considered, involving the convergence of two targets to within 15 m, followed by parallel motion over a distance of 190 m and subsequent divergence (Fig. 6). Experiments were conducted with identical Signal-to-Noise Ratio (SNR) values for both targets: (14 dB, 14 dB) and (15 dB, 15 dB), as well as for different values (14 dB, 15 dB).

Figures 7 and 8 present the divergence probabilities ($P_{\text{divergence}}$), obtained using the known JPDAF algorithm. From the results obtained, it follows that the JPDAF algorithm cannot be applied at an SNR of (14 dB, 14 dB) for the investigated false alarm probability values. When increasing the SNR to 15 dB (Fig. 8), at a false alarm rate of $F = 10^{-4}$, the probability of track loss due to gate divergence ($P_{\text{divergence}}$) is approximately 16%. This is 8 times higher than the indicator for the scenario with simple intersecting trajectories (Fig. 4), confirming the significant complexity of the selected motion conditions.

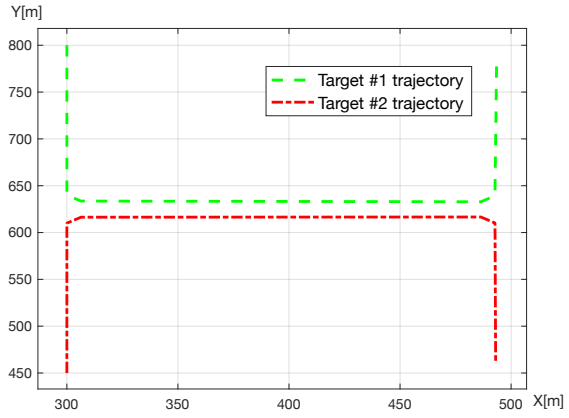

Fig. 6. Trajectories of two targets.

The simulation results for the AA-JPDAF algorithm for the considered motion scenario are shown in Figs. 9 and 10.

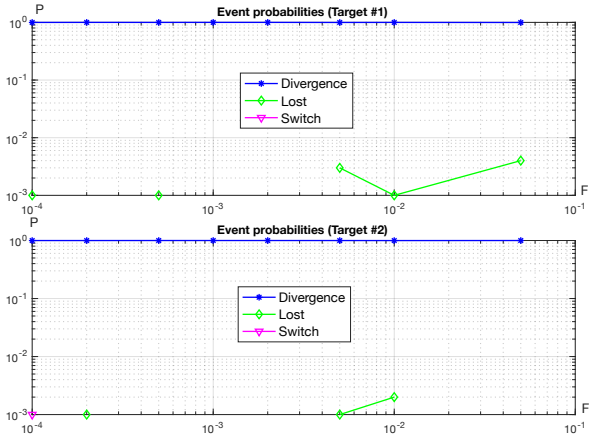

Fig. 7. Tracking event probabilities for AA-JPDAF, SNR (14 dB, 14 dB).

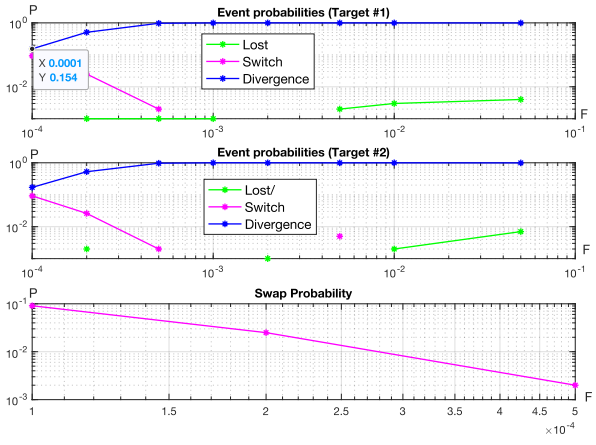

Fig. 8. Tracking event probabilities for AA-JPDAF, SNR (15 dB, 15 dB).

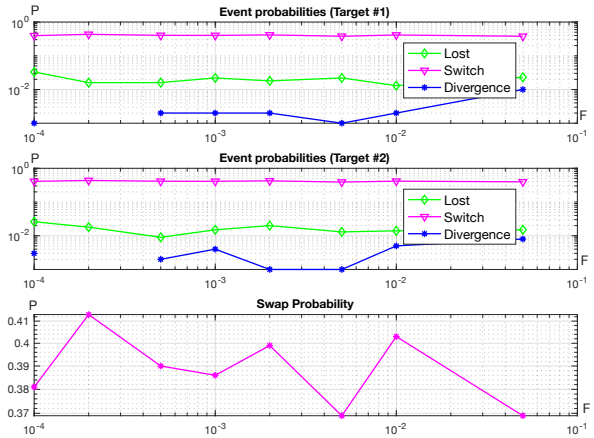

Fig. 9. Tracking event probabilities for AA-JPDAF, SNR (14 dB, 14 dB).

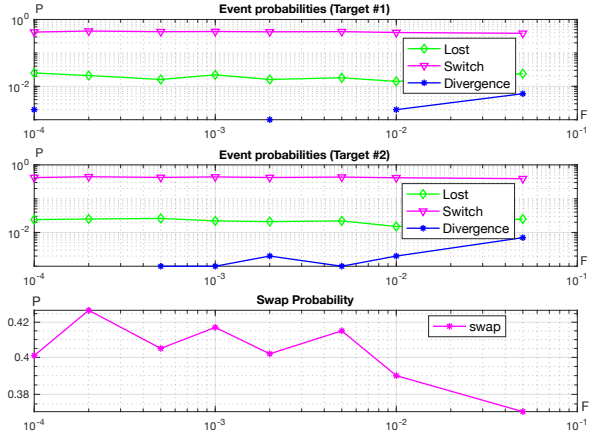

Fig. 10. Tracking event probabilities for AA-JPDAF, SNR (15 dB, 15 dB).

The obtained data confirm the high effectiveness of the developed approach:

- for both SNR values of 14 dB and 15 dB, the gate divergence probability $P_{\text{divergence}}$ does not exceed 0,8%, while the track loss probability P_{lost} is 2,6% across the entire range of false alarm rates ($F = 10^{-4} \ldots 5 \cdot 10^{-2}$);
- the switching probability P_{switch} ranges from 36.4% to 43.3% for an SNR of 14 dB and from 38.5% to 45% for an SNR of 15 dB.

The mutual swap probabilities P_{swap} are recorded within the limits of 34.8% to 41.3%.

The experimental results for the case of different target SNR values (14 dB, 15 dB) are presented in Fig. 11. The use of amplitude information under unequal target energy conditions (1 dB difference) enabled the following performance characteristics:

- the probability of gate divergence ($P_{\text{divergence}}$) remains consistently low (less than 0.2%), while the probability of track loss (P_{lost}) fluctuates within the range of 1.3% – 3.5%, even at a false alarm rate of $F = 5 \cdot 10^{-2}$;
- the probability of switching (P_{switch}) has significantly decreased to a range of 26.5% – 34.7%, which is

on average 10% better than in scenarios with identical target SNR values.

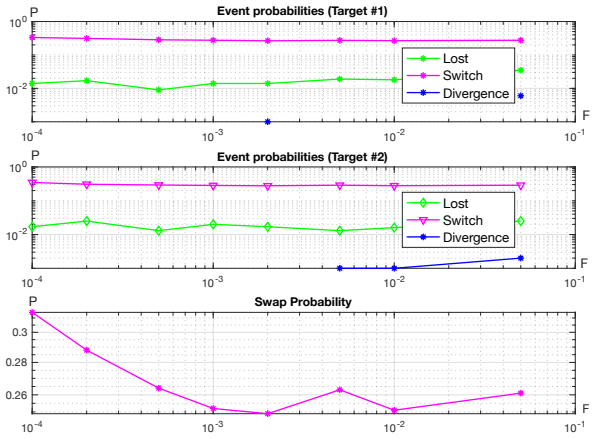

Fig. 11. Tracking event probabilities for AA-JPDAF, SNR (14 dB, 15 dB).

A trend toward a decrease in the mutual swap probability (P_{swap}) was recorded, dropping from 31.4% to 25% – 26% as the clutter intensity increased.

Consequently, the use of the developed AA-JPDAF multitarget tracking algorithm for FMCW radar data makes it possible to increase the tracking effectiveness compared to the conventional JPDAF algorithm in the presence of a significant number of false reports.

Conclusions

In this work, a multitarget tracking algorithm for FMCW radar data, AA-JPDAF, has been developed, that exploits amplitude information (decision statistics) from the output of the optimal primary signal processing receiver. For the considered model examples, results demonstrate that the developed AA-JPDAF algorithm, which uses decision statistics, allows for a significant improvement in tracking effectiveness in environments characterized by a high level of false alarm probability, as well as in complex scenarios involving the motion of closely spaced targets.

The algorithm maintains the spatial localization of objects and exhibits low values for the probabilities of gate expansion and track loss, which is critical for practical systems. The probability of mutual trajectory swapping for closely spaced targets decreases if they are characterized by different SNR levels.

References

[1] W. Khawaja, M. Ezuma, V. Semkin, F. Erden, O. Ozdemir, and I. Guvenc. (2025). A Survey on Detection, Classification, and Tracking of AAVs Using Radar and Communications Systems. *IEEE Communications Surveys and Tutorials*, early access, doi: 10.1109/COMST.2025.3554613.

[2] Y. Mekdad et al. (2023). A Survey on Security and Privacy Issues of UAVs. *Computer Networks*, Vol. 224, Art. no. 109626, doi: 10.1016/j.comnet.2023.109626.

[3] Y. Alqudsi and M. Makaraci. (2025). UAV swarms: Research, challenges and future directions. *Journal of Engineering and Applied Science*, Vol. 1, doi: 10.1186/s44147-025-00582-3.

[4] A. N. Sayed, O. M. Ramahi, and G. Shaker. (2024). Frequency-Modulated Continuous-Wave Radar Perspectives on Unmanned Aerial Vehicle Detection and Classification: A Primer for Researchers with Comprehensive Machine Learning Review and Emphasis on Full-Wave Electromagnetic Computer-Aided Design Tools. *Drones*, Vol. 8, No. 8, Art. no. 370, doi: 10.3390/drones8080370.

[5] I. K. Kapoulas, A. Hatziefremidis, A. K. Baldoukas, E. S. Valamontes, and J. C. Statharas. (2023). Small Fixed-Wing UAV Radar Cross-Section Signature Investigation and Detection and Classification of Distance Estimation Using Realistic Parameters of a Commercial Anti-Drone System. *Drones*, Vol. 7, No. 1, Art. no. 39, doi: 10.3390/drones7010039.

[6] M. I. Skolnik. (2008). *Radar Handbook*, 3rd ed. New York, NY, USA: McGraw-Hill, 1352 p.

[7] Y. Bar-Shalom, X. R. Li, and T. Kirubarajan. (2011). *Tracking and Data Fusion: A Handbook of Algorithms*. Storrs, CT, USA: YBS Publishing, 1250 p.

[8] L. A. Kuzmin. (2000). *Digital radar. Introduction to theory [Tsifrovaya radiolokatsiya. Vvedenie v teoriyu]*. Kiev, Ukraine: KVITs.

[9] O. S. Neuimin and S. Y. Zhuk. (2014). Sequential detection of target trajectory using the decision statistics of pips. *Radioelectronics and Communications Systems*, Vol. 57, pp. 262–273, doi: 10.3103/S0735272714060041.

[10] T. V. Malenchyk and S. Ya. Zhuk. (2024). Algorithm for Sequential Detection of Trajectory of Small Sized UAV by FMCW Radar According to Strongest Neighbor Criterion. *Visnyk NTUU KPI Seriia – Radiotekhnika Radioaparatobuduvannia*, No. 98, pp. 23–29, doi: 10.20535/RADAP.2024.98.23-29.

[11] S. Ya. Zhuk, T. V. Malenchyk, O. S. Neuimin, and O. Myronchuk. (2022). Adaptive Radar Tracking Algorithm for Maneuverable UAV with Probabilistic Identification of Data Using Coordinate and Amplitude Characteristics. *Radioelectronics and Communications Systems*, Vol. 65, No. 10, pp. 503–516, doi: 10.3103/S073527272212007X.

[12] B.-N. Vo, M. Mallick, Y. Bar-Shalom, S. Coraluppi, R. Osborne III, R. Mahler, and B.-T. Vo. (2015). Multitarget Tracking, in *Wiley Encyclopedia of Electrical and Electronics Engineering*, J. G. Webster, Ed. Hoboken, NJ, USA: Wiley, doi: 10.1002/047134608X.W8275.

[13] D. K. Barton. (2005). *Radar System Analysis and Modelling*. Norwood, MA, USA: Artech House, 549 p.

[14] Y. Bar-Shalom, X. R. Li, and T. Kirubarajan. (2001). *Estimation with Applications to Tracking and Navigation: Theory, Algorithms and Software*. New York, NY, USA: Wiley, DOI:10.1002/0471221279.

[15] X. R. Li and Y. Zhao. (2006). Evaluation of estimation algorithms — Part I: Incomprehensive measures of performance. *IEEE Transactions on Aerospace and Electronic Systems*, Vol. 42, No. 4, pp. 1340–1358, DOI: 10.1109/TAES.2006.314576.

[16] S. Blackman and R. Popoli. (1999). *Design and Analysis of Modern Tracking Systems*. Norwood, MA, USA: Artech House, 1230 p.

[17] H. You, X. Jianjuan, and G. Xin. (2016). *Radar Data Processing with Applications*. Singapore: John Wiley & Sons Singapore Pte. Ltd., doi: 10.1002/9781118956878.

[18] R. P. S. Mahler. (2007). *Statistical Multisource-Multitarget Information Fusion*. Norwood, MA, USA: Artech House, 888 p.

[19] Y. Huang, T. L. Song, and D. H. Cheagal. (2019). Markov Chain Realization of Multiple Detection Joint Integrated Probabilistic Data Association. *Sensors*, Vol. 19, No. 1, Art. no. 112, doi: 10.3390/s19010112.

[20] S. Liang, Y. Zhu, and H. Li. (2022). Evolutionary Optimization Based Set Joint Integrated Probabilistic Data Association Filter. *Electronics*, Vol. 11, No. 4, Art. no. 582, doi: 10.3390/electronics11040582.

Алгоритм супроводження кількох цілей з сумісним ймовірнісним ототожненням даних з використанням координатної і амплітудної інформації

Ковтун І. С., Жук С. Я.

Широке застосування малорозмірних безпілотних літальних апаратів (БПЛА) обумовлює актуальність задачі їхнього супроводження в умовах, коли об'єкти перебувають на малих відстанях, а також їхні траєкторії перетинаються. Сучасним засобом виявлення і супроводження малорозмірних БПЛА є радар з частотно-модульованим безперервним випромінюванням (Frequency-Modulated Continuous-Wave, FMCW), який дозволяє суттєво зменшити пікову потужність випромінювання, а отже – знизити енергоспоживання та покращити масо-габаритні й вартісні характеристики системи. Малорозмірні БПЛА мають екстремально низькі значення ефективної поверхні розсіювання. Збільшення дальності виявлення малорозмірних БПЛА FMCW радаром може бути досягнуто шляхом зниження порога виявлення, що однак призводить до значного зростання ймовірності хибної тривоги. Для підвищення ефективності супроводження кількох цілей за даними FMCW радара при наявності значної кількості хибних відміток в роботі розроблено алгоритм — фільтр з сумісним ймовірносним ототожненням даних з використанням амплітудної інформації (Amplitude-Aided Joint Probabilistic Data Association Filter, AA-JPDAF), в якому в якості додаткової інформації запропоновано використовувати вирішальні статистики (амплітудну інформацію) з виходу оптимального приймача первинної обробки сигналів. Ця інформація використовується на етапі ототожнення відміток за траєкторіями на основі методу спільного ймовірнісного ототожнення даних (Joint Probabilistic Data Association, JPDA). Оцінювання параметрів руху цілей за кожною траєкторією відбувається з використанням розширеного фільтра Калмана (Extended Kalman Filter, EKF). Аналіз алгоритму AA-JPDAF і його порівняння з відомим алгоритмом JPDAF проведено шляхом статистичного моделювання для сценаріїв із перетином траєкторій та тривалим паралельним рухом цілей на малих відстанях.

Ключові слова: FMCW радар; БПЛА; багатоцільове супроводження; хибні відмітки; спільне ймовірнісне ототожнення даних; фільтр Калмана; апостеріорна ймовірність; вирішальна статистика; відношення сигнал/шум; зрив супроводження